Cavity-ring-down spectroscopy of the heavy ozone isotopologue 18O3: Analysis of a high energy band near 95% of the dissociation threshold

Semen Vasilchenko, Alain Barbe, Evgeniya Starikova, Samir Kassi, Didier Mondelain, Alain Campargue, Vladimir Tyuterev

Cavity-ring-down spectrum of the heavy ozone isotopologue $^{18}O_3$: analysis of high energy band near 95% of the dissociation threshold

Semen Vasilchenko[1,3], Alain Barbe[2], Evgeniya Starikova[1,3*], Samir Kassi[4], Didier Mondelain[4], Alain Campargue[4], and Vladimir Tyuterev[3,2]

[1]*V. E. Zuev Institute of Atmospheric Optics SB RAS, av. 1, Akademician Zuev square, 634055 Tomsk, Russia*
[2]*Groupe de Spectrométrie Moléculaire et Atmosphérique, UMR CNRS 7331, UFR Sciences Exactes et Naturelles, BP 1039 - 51687 Reims Cedex 2, France*
[3]*Laboratory of Quantum Mechanics of Molecules and Radiative Processes, Tomsk State University, 36 Lenin Avenue, 634050 Tomsk, Russia*
[4] *Université Grenoble Alpes, CNRS, LIPhy, 38000 Grenoble, France*

Running head:
Number of pages:
Number of figures: 4
Number of Tables: 2

Keywords: Ozone, Isotopologue, Dissociation threshold, Cavity-ring-down spectroscopy, Effective Hamiltonian model, Line lists

Submitted to JQSRT
* Corresponding author: e-mail: starikova_e@iao.ru

1. Introduction

The isotopic anomalies in ozone formation discovered in the atmosphere and laboratory settings [1-10] which are not yet fully understood, and the long-term issues related to isotopic exchange reactions [11-17] are among well-recognized incentives for in-depth studies of infrared spectra, vibration-rotation energies and transitions of this unstable species.

The most of recent studies of high-resolution spectra were devoted to the main isotopologue of ozone $^{16}O_3$, involving both *ab initio* calculations [18-22] and analyses of laboratory experiments using Fourier transform spectroscopy (FTS) [23-28] (and references therein) linked to the quest of intensity consistency among the absorption bands. The corresponding line lists, particularly for the spectral range below 5400 cm^{-1} have been updated in the last releases of HITRAN [29], GEISA [30] databases and in S&MPO ("Spectroscopy and Molecular Properties of Ozone") information system [22,28,31] also accessible from the VAMDC internet portal [32].

At higher energy range, the absorption intensities of vibrational bands rapidly decrease at increasing wavenumbers. Highly sensitive laser techniques [33-38] allowed recording weaker bands towards the dissociation threshold estimated at D_0 ~8560 cm^{-1} [39,40] with sufficient S/N ratio.

The $^{16}O_3$ spectra in the 5850-8000 cm^{-1} region was investigated in the series of the previous works [34-38] (and references therein) by cavity-ring-down spectroscopy (CRDS) resulting in assignment and analyses of thirty-two ro-vibrational bands. A good agreement of the observed band origins with *ab initio* calculations [19,41,42] has permitted resolving a long-standing controversy concerning the shape of the potential energy surface (PES) at the transition energy state range (the absence of the "reef structure" [40,41,43] between the molecule and the dissociation fragments).

Reviews of recent works on measurements and analyses of isotopic ^{18}O-enriched ozone spectra with one ($^{16}O^{16}O^{18}O$ / $^{16}O^{18}O^{16}O$) or two ($^{16}O^{18}O^{18}O$ / $^{18}O^{16}O^{18}O$) substitutions can be found in [44-48] and a complete list of references to previous works at the S&MPO web sites http://www.ozone.univ-reims.fr and http://ozone.iao.ru.

The spectra of the heavy $^{18}O_3$ isotopologue in the FTS range below 5000 cm^{-1} were studied in [49-52], whereas CRDS spectra were measured and analyzed [53-58] at higher wavenumber in the interval 5800-7920 cm^{-1}. In our recent works on the $^{16}O_3$ [38,59], we were able to further extend the spectral range using external cavity diode laser (ECDL) instead of a series of fibered distributed feedback (DFB). This allowed for a more efficient light injection into the CRDS cell and thus for an improved sensitivity with a routine noise equivalent absorption, α_{min}, on the order of a few 10^{-11} cm^{-1}. As a result, the highest ro-vibrational energy level determined from the analysis was only 3.3 % below the dissociation threshold.

The present study aims at applying the same techniques for $^{18}O_3$ spectra in the wavenumber range at about 95% of the dissociation threshold. The reader is referred to the detailed discussions in the first publication [38] concerning the importance of highly excited ro-vibrational states and transitions at this energy range in various fields of science. Another motivation of the near infrared spectroscopy of $^{18}O_3$ is that vibrational patterns in the considered interval are shrunk down by about 400-450 cm^{-1} for the heavy isotopologue compared to $^{16}O_3$. The observation in the same wavenumber range can thus provide information for upper vibrational states or combination bands of ozone, which were not yet experimentally known for the main species $^{16}O_3$. Consequently, the analysis of transition will probe extended geometries of the potential energy surface, giving supplementary information for the validation of *ab initio* calculations.

It has been already found [57] that, contrary to the low energy range, the isotopic shifts of the band origins between $^{16}O_3$ and $^{18}O_3$ isotopologues are irregular, even though the change in masses is small and homogeneous. Ro-vibrational lines in the considered range are

even weaker (of the order of 10^{-29} cm/molec) than for $^{16}O_3$ range. This makes analyses of spectra a non-trivial task that is complicated by the presence of much stronger diffuse features of electronic hot bands [60,61] of the Wulf system.

2. Experimental.

In cavity ring-down spectroscopy, the absorption coefficient, α, at the frequency ν is directly calculated from the exponential decay time, τ, of the electromagnetic field inside a high finesse cavity :

$$\alpha(\nu) = \frac{1}{c}\left(\frac{1}{\tau} - \frac{1}{\tau_0}\right),$$

where c is the light velocity and τ_0 is the ring-down time in the empty cavity due to the mirrors transmissivity, diffraction losses, scattering, etc.

The CW-CRDS spectrometer is described in detail in [62]. In this work we did not use a femtosecond laser frequency comb for laser frequency reference, a Fizeau wavelength meter (High Finesse WS-U-30 IR, 5 MHz resolution, 20 MHz accuracy) was used for laser frequency measurements.

The reader is referred to [38] for a detailed description of ozone generation and spectra recording process here we briefly mention key points.

A silent discharge (12 kV, 400 Hz) was used for ozone generation [63]. CRDS cell, vacuum compartment, and glass flask of the ozone generator were filled with oxygen isotopologue $^{18}O_2$ (ISOTEC, min 99% ^{18}O atoms) to a pressure of P_0 = 60 Torr at room temperature. Then the generator flask was immersed into a Dewar vessel filled with liquid nitrogen, and the discharge was turned on for a few minutes. As a result of oxygen transformation into ozone ($3O_2 \rightarrow 2O_3$), the total pressure in the system gradually decreased for several minutes and the ozone froze in the ozone generator flask. The discharge was turned off at a residual pressure of 0.4 Torr. After removing the Dewar's vessel, the ozone evaporated and the pressure of pure ozone in the system was set close to $(2/3)P_0 \approx 40$ Torr.

The ozone decay can be estimated from the rate of increase in the total pressure in the system. Assuming an increase in the total pressure by 1 Torr to correspond to 2 Torr decrease in the partial pressure of ozone $2O_3 \rightarrow 3O_2$. The partial pressure of ozone can be found from the total pressure P measured at each spectral point $P_{O_3} = 2(P_0 - P).$, where P is the total pressure at a given spectral point read by a pressure gauge. So, in the region of interest (7940 – 7985 cm^{-1}) an increase in the total pressure from 41.1 to 42.4 Torr corresponds to the partial pressure of ozone linear decrease from 37.8 to 35.2 Torr at a rate of 0.24 Torr/h during near 11h of spectra recording.

In total in this study 16 spectra of $^{18}O_3$ were recorded in the spectral range from 7920 to 8400 cm^{-1} with a typical sensitivity of 3×10^{-11} cm^{-1} by absorption coefficient. In the present study, we focus on the region between 7920 and 7985 cm^{-1} because just below and after this interval the absorption is dominated by much stronger diffuse features of the vibronic hot bands of the Wulf system [64]. The strongest cold bands of the Wulf singlet-triplet transitions fall to the range 9500-12500 cm^{-1} and have been studied in a series of works [65-68] (and references therein).

In our spectral range the hot ro-vibronic bands correspond to transition between excited vibrational levels of the electronic ground state $X^1A_1(v_1v_2v_3)$ and the triplet electronic state $^3A_2(000)$. At lower wavenumbers, the lines of ro-vibronic hot bands of $^{18}O_3$ have been assigned in [60,61], but there is no reliable theoretical or experimental information in the literature on the ro-vibronic transition of hot band $X^1A_1(v_1v_2v_3)$ <-$^3A_2(000)$ for $^{18}O_3$ above 7920 cm^{-1}.

Spectra were calibrated, thanks to 4 strong HF lines present in the spectra as impurity lines HITRAN database [69] and declare position uncertainty for those lines between 0.0001

and 0.001 cm^{-1}. Conservatively, we estimate the average uncertainty of ozone line positions at the level of 0.002 cm^{-1}.

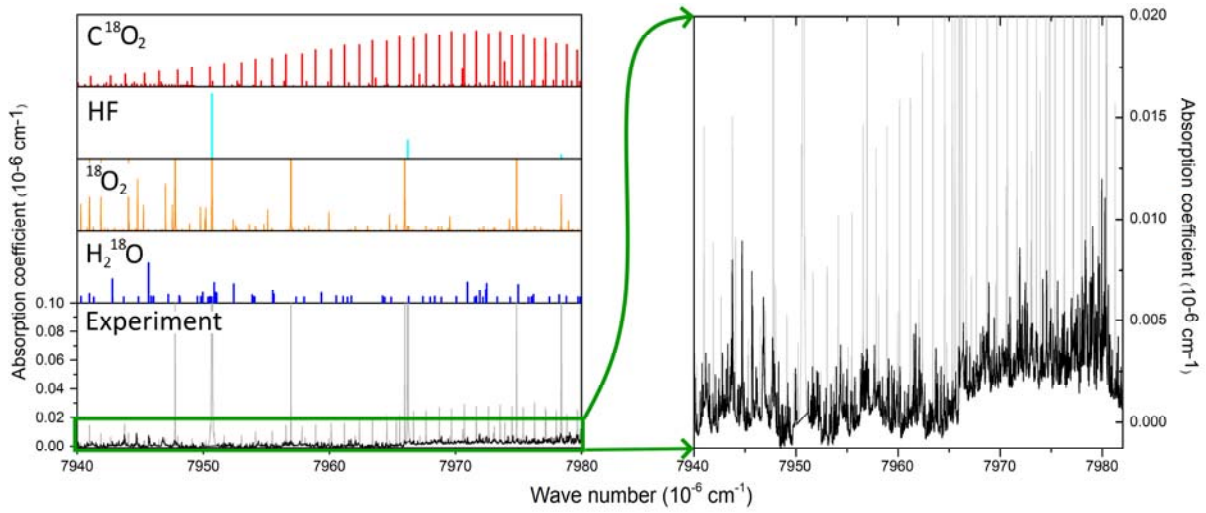

Fig 1. *Overview of the CRDS recordings of $^{18}O_3$ between 7940 and 7985 cm^{-1}. Left panels: Due to the weakness of the ozone spectrum, the recorded spectrum (lower panel) is dominated by impurity lines. The spectrum of ^{18}O-enriched oxygen was recorded at the pressure of 20 Torr, line lists of $H_2{}^{18}O$, $C^{18}O_2$ and HF were adopted from W2020 [70], Ames-2016 [71] and HITRAN [69] respectively. CO_2 lines were shifted by 0.0275 cm^{-1} to be consisted with measured positions. CRDS spectrum of ozone was normalized at the ozone pressure of 36 Torr. Right panel: Enlargement of the ordinate scale by a factor of about 20 showing ozone bands after removing strong impurity lines corresponding to identified impurities.*

According to first principle predictions from the *ab initio* PES [19] (see the next Section for details), the most plausible candidate for the ro-vibrational band in this range is $7\nu_1+\nu_3$ with the band head about 7980 cm^{-1}. To identify the lines that could belong to this band two spectra were used. An important difficulty of the spectrum treatment was related to the superposition of many impurity lines to the targeted ozone spectrum. $^{18}O_2$, $H_2{}^{18}O$, $C^{18}O_2$, and HF were identified as impurities. In the region of the $7\nu_1+\nu_3$ band impurity lines strongly dominate, additionally ^{18}O isotope enriched sample of the gas produces rare isotopologues of impurities which were difficult to identify and are excluded from the fit. To eliminate absorption features due to impurities, overlapping ozone spectra were normalized to the same ozone partial pressure and two spectra of $^{18}O_2$ at pressures of 10 and 20 Torr were recorded in the region. Comparing the relative intensity of the lines among several spectra one can sort features into O_3 and impurities.

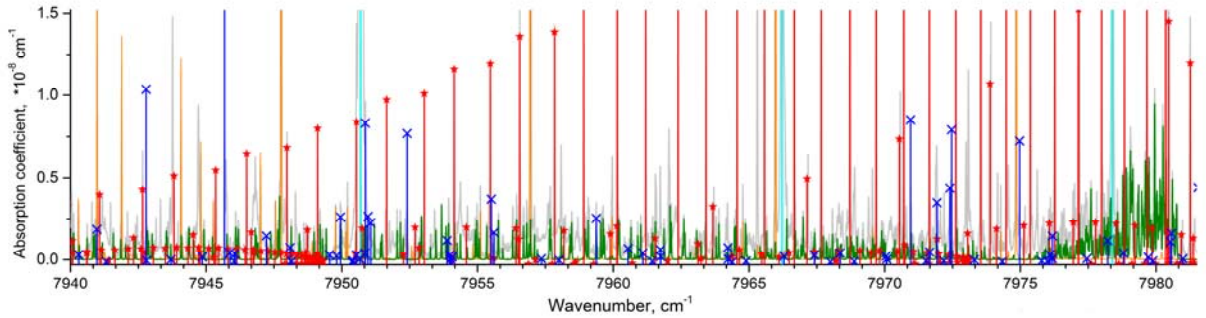

Fig 2. *Blown-out recorded spectrum in the 7940-7985 cm^{-1} range. Gray line corresponds to recorded $^{18}O_3$ spectrum. Green line corresponds to the simulation of the ozone $7\nu_1+\nu_3$ band with the strongest features belonging to electronic transitions (??). Dominating impurity lines are marked by red stars*

($C^{18}O_2$) crosses ($H_2{}^{18}O$), cyan sticks (HF), and orange line corresponds to scaled recorded $^{18}O_2$ spectrum.

Spectra were normalized to the constant partial pressure of ozone for ease of fit. They were fitted using Voigt profile, Gaussian width was fixed to the calculated value.
During the recordings, the molar fraction of the impurities grows according to the ozone decomposition, desorption, or chemical reactions with the walls of the setup. Therefore, for the band head an additional spectrum was recorded with minimal impurity abundance (see Fig 1).

III. Analysis and results

The vibrational assignment relies on variational predictions of band origins using *ab initio* potential energy surface of Ref. [19] and on the subsequent decomposition of the corresponding *ab initio* wavefunction in the normal mode basis set using the contact transformation (CT) method. To this end, we used MOL_CT program suite [72,73].

In case of ozone molecule, the parallel bands activated due to the component of the dipole moment, which is parallel to the a-axis of the principal inertia moment (A-type bands) are usually much stronger than the perpendicular bands. This was shown both *ab initio* calculations [21,22] and by many analyses of experimental spectra in the past [25-28, 34-38]. Our previous studies of CRDS spectra have clearly shown that only parallel bands with the selection rules $\Delta\upsilon_3 = odd$ and $\Delta K_a = even$ [74] were assignable the high-energy range. In terms of symmetry, the situation for $^{18}O_3$ is similar to the case of $^{16}O_3$, and the reader can find more detailed discussions in the previous works [38].

The comparison with theoretical predictions clearly show that the most plausible candidate for the typical parallel type band shape appearing at the right-hand Figs 1 and 2 can be assigned as $7\nu_1+\nu_3$ with the calculated origin near 7973 cm^{-1}. The coefficient 0.84 of the principal terms (7.0.1) in the normal mode decomposition of the upper state wavefunction clearly dominate other basis set contributions. This is confirmed by calculations from *ab initio* PES of [19] and from the PES of [75] which had been empirically optimised using fine tuning fit to experimental levels of $^{16}O_3$ below 5000 cm^{-1}. As in previous studies [21,36], to help the assignment, the ro-vibrational J= 1 and J= 2 levels were computed from the PES and used to determine theoretical values of A_V, B_V and C_V rotational constants.

We have applied a combination of similar methods and program codes (MULTIFIT [76], ASSIGN [77] and GIP [78]) for the assignment of rotational quantum numbers, and for iterative calculations and empirical fits of energy levels and transitions as was described in our previous paper devoted to the analyses of $^{16}O_3$ CRDS spectra [38], where the reader can find more detail concerning the definitions of effective models and related references. As in the case of $^{16}O_3$, the analysis was quite laborious and complicated due to the following reasons:

(a) The vibration-rotation transitions of $^{18}O_3$ appear to be are extremely weak, much weaker than $^{16}O_3$ transitions in the same range near the dissociation threshold. The absorption is dominated by electronic hot bands and by lines of hardly avoidable impurities. The latter ones have line intensities which are stronger by several orders of magnitude even at very small abundance.

(b) The number of such strong lines due to impurities was very large and difficult to be completely removed (as is seen in Figs 1, 2). After several unfruitful attempts, we were able to find out rotational K_a = 4 series using ASSIGN code [77] and to proceed by successive assignments. This was only possible after the identification of a large part of impurity lines using two spectra records with different partial pressures of ozone in the cell (section II).

(c) As far as the ozone analyses advance towards higher energies (see figure 7 of the review paper [36]), the errors of the fits for line positions and intensities using effective Hamiltonian (EH) and effective dipole transition moment (EDTM) models generally increase. As discussed in [38], the observed-calculated deviations during successive iterations of assignments do not follow regular slopes, when plotting these deviations versus J for a given K_a quantum number.

Finally, we were able to assign 259 vibration-rotation transitions of the $7\nu_1+\nu_3$ band, corresponding to 171 upper state energy levels, with J_{max} = 25 and $K_{a\ max}$= 8 (see Table 1). The full set of experimental levels is given in the Supplementary materials (Table S1). The root-mean-square (*rms*) deviation 0.016 cm^{-1} for the fit of line positions is similar to that obtained for the bands of $^{16}O_3$ in the same spectral range [38]. Some attempts to include dark states, predicted from the PES [19], permitted to slightly improve the *rms* deviation of the fit, but were not sufficiently reliable to be included in the final analysis.

As in previous studies, we have determined two effective dipole transition moment parameters of the observed band using experimentally measured intensities for 127 relatively isolated lines. These parameters correspond to main terms in the EDTM expansion [79]

$$^{(V^u)(V^l)}\tilde{\mu}_Z^{(A)} = d_1^A \varphi_z + d_2^A \left\{\varphi_z, \mathbf{J}^2\right\},$$

where the notation $\{X,Y\} = XY + YX$ stands for an anti-commutator, φ_α are direction cosines for the Eckart molecular fixed frame and J^2 is the square of total angular momentum.

The corresponding statistics of the line intensity fit using EH and EDTM parameters with the *rms* intensity deviation of 13.2% are given in Table 1 and the full comparison between measured and calculated intensities is given in the Supplementary materials (Table S2).

Table I. Spectroscopic parameters and fit statistics for the $7\nu_1+\nu_3$ band of $^{18}O_3$ band centred at 7974 cm^{-1}.

(i) Spectroscopic parameters (cm^{-1}) [a]			*(iii)* Statistics for line positions	
Upper states		(7,0,1) ≡ (B_1, 105)	J_{max}	29
E^{VV}		7974.0228_4 (27)	K_{amax}	8
A_V-(B_V+C_V)/2		2.72443_0 (22)	Number of transitions	259
(B_V+C_V)/2		0.3536940_1 (68)	Number of levels	171
(B_V-C_V)/2		0.021887_5 (43)	*rms*(cm^{-1})	0.016
Δ_K	$\times10^3$	0.1909_9 (34)	*(iv)* Statistics for line intensities	
Δ_{JK}	$\times10^5$	0.261_7 (30)	J_{max}	25
δ_J	$\times10^6$	0.144_7 (38)	K_{amax}	8
(ii) Dipole transition moment parameters (Debye)			Number of transitions	127
$d_1^{(A)}$	$\times10^5$	0.2633_8 (24)	*rms* (%)[a]	13.2
$d_2^{(A)}$	$\times10^{10}$	-0.95_0 (32)	S_v = 1.19×10^{-26} cm/molecule at 296 K[b]	

Notes: [a] Watson notations [80] for A-type reduced EH parameters in I^r representation. All higher order centrifugal distortion parameters quoted in [49] were held fixed to their ground state values. [b] Sum of intensities in the calculated line list (477 lines).

These parameters were used to generate a set of 477 calculated transitions of the $7\nu_1+\nu_3$ band reported in the Supplementary materials (Table S3). The calculated set was limited to transitions which reach experimentally determined upper state levels. Line positions were empirically corrected according to the experimental value of the upper energy levels. Line

intensities were computed using the fitted EDM parameters and the wavefunctions corresponding to the EH of Table I. A comparison of simulated absorption coefficient using our line list with experimentally recorded spectra (including impurity lines) in the regions of the *P*- and *R*-branched of the $7\nu_1+\nu_3$ band show a satisfactory agreement accounting for assignable series of lines (Figs 3a and 3b).

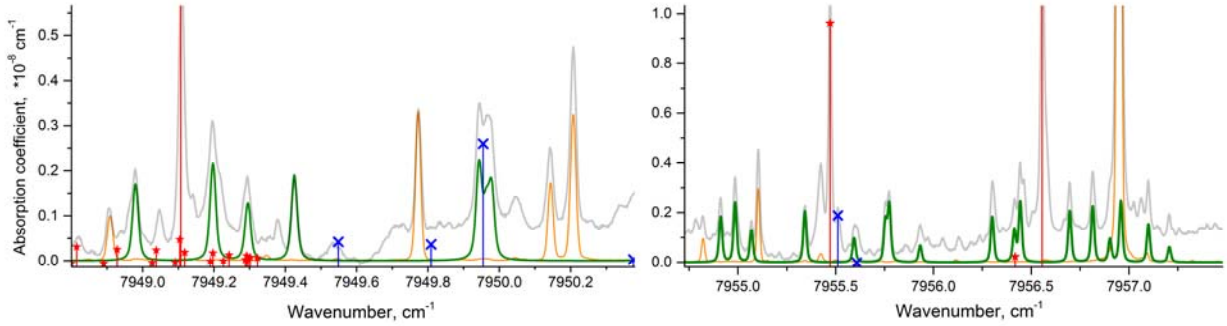

Fig 3a. *Example of comparison of CRDS and simulated spectra in the P-branch region in the $7\nu_1+\nu_3$ band of $^{18}O_3$. Gray line corresponds to recorded $^{18}O_3$ spectrum. Impurity lines are marked by red stars ($C^{18}O_2$), crosses ($H_2{}^{18}O$), cyan sticks (HF), orange line corresponds to scaled $^{18}O_2$ spectrum recorded at 20 Torr.*

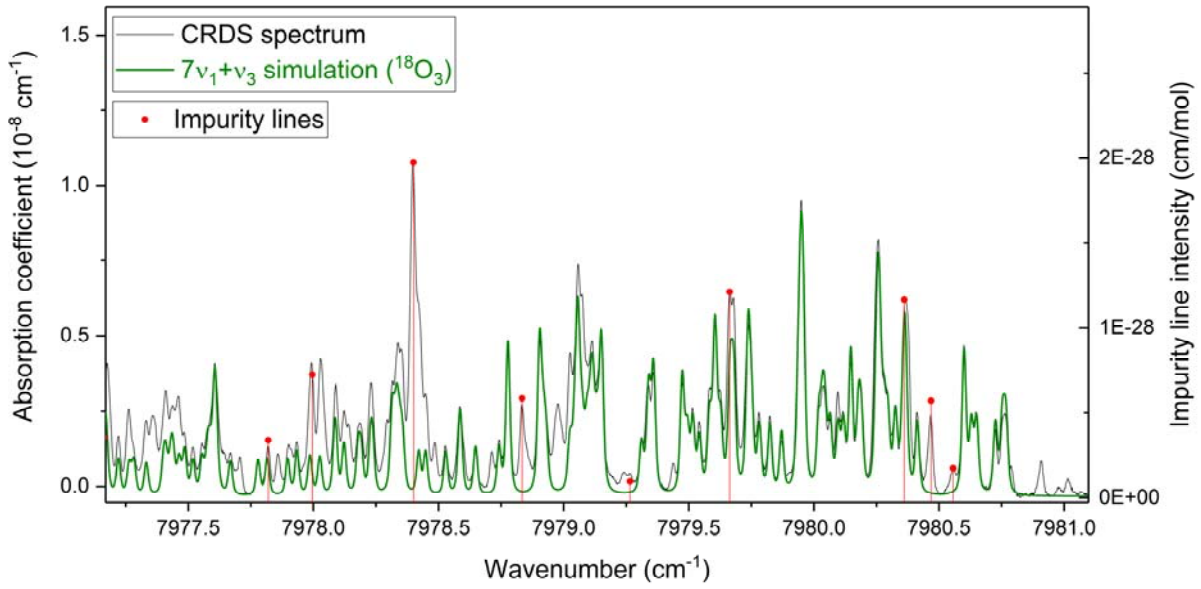

Fig 3b. *Comparison of CRDS and simulated $^{18}O_3$ spectra in the R-branch near the band head of $7\nu_1+\nu_3$*

Finally, Table II gives the comparison for the band origin and rotational constants between observations and theoretical predictions. As for $^{16}O_3$, these comparisons show a very good agreement for this high energy range

Table II. Comparison of experimentally determined band centers and upper state rotational constants with theoretical predictions using *ab initio* [19] and empirical [75] PESs.

Upper state	Exp. (TW)	*ab initio* [19]	Exp.-Calc.	empirical PES [75]	Exp.-Calc.
(7,0,1)	7974.023	7972.771	1.252	7975.349	-1.326
A_V	3.078	3.068	0.010	3.070	0.008
B_V	0.376	0.366	0.008	0.374	0.002

C_V	0.332	0.297	0.005	0.331	0.001

Notes: All values are given in cm^{-1}. TW = This work.

III. Conclusion

Experimental information on the isotopic behavior of the vibration-rotation energy level patterns near the dissociation threshold is of major importance "*for the checking the shape of the PES in the transition states region and verifying quantum-mechanical resonance calculations"* [9]. This in turn can be essential for verifying the dynamical models in the study of anomalous isotopic effects in the ozone formation. However, a direct experimental access to these quantum states is an extremely challenging task. The intensities of ro-vibrational bands in the ranges approaching the dissociation threshold fall down very rapidly as is illustrated in the log-scale scheme of Fig. 4, where all previous measurements are compiled together with the results of the present work. With respect to the fundamental bands, the line intensities drop down by about nine orders of magnitude. This requires a very high sensitivity of the experimental setup that was achieved in the present work.

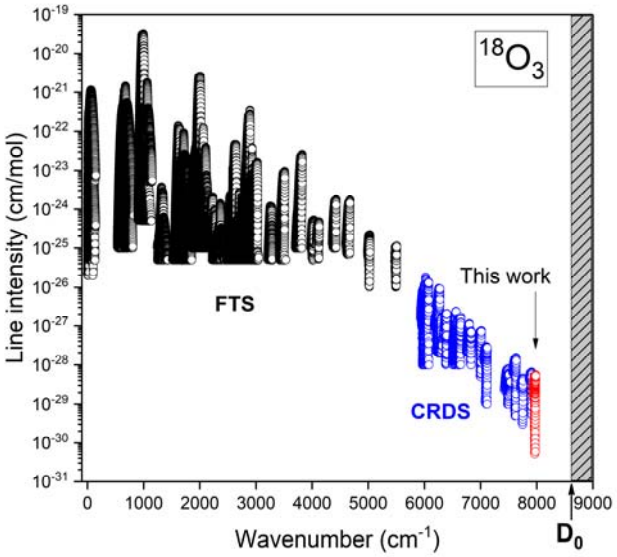

Fig 4. *Overview of the line lists of the analyzed ro-vibrational bands of $^{18}O_3$. Up to 5200 cm^{-1}, line list (black circles) was obtained mainly from FTS measurements [49-52] complemented by JPL catalogue in MW region [81]. The CRDS data of Refs. [53-59] cover the 5850-7900 cm^{-1} region (blue circles) while the most excited $7\nu_1+\nu_3$ band above 7900 cm^{-1} is studied in this work. The dissociation threshold $D_0(^{18}O_3)$ is indicated.*

In the spectral range of this study the estimated sum of intensities due to ro-vibrational transitions (evaluated from our list (Table S3) and that of ref [38]) is about four-to-five times weaker than for the main $^{16}O_3$ isotopologue. This can be explained by the fact that vibrational levels of the heavy isotopologue shrink down by about 400 cm^{-1} compared to the lighter one because of the isotopic shift, and the PES supports larger number of bound ro-vibrational states. Consequently, spectral transitions of the heavy isotopologue probe higher vibration excitations in different directions of the nuclear displacements. The ro-vibrational band $7\nu_1+\nu_3$ of $^{18}O_3$ observed and assigned in this work corresponds to vibrational motion of the upper (7.0.1) state that simultaneously probe seven-fold excitation of the symmetric stretch plus one excitation of asymmetric stretch. Analyses of *ab initio* wavefunctions [42] show that despite a significant mixing of the basis functions near D_0, some vibrational states keep a pronounced

normal mode character for all isotopologues. This is the case of vibrations corresponding to large symmetric stretch excitations $n\nu_1$ because the energy gapes increase towards the top of the polyads.

Ro-vibrational patterns experimentally determined in this work extend up to 8355.3 cm^{-1} ($[J,K_a,K_c](v_1.v_2.v_3)$= [26,7,20](7.0.1) level of $^{18}O_3$ at Table S1), which is the highest so far measured ro-vibrational level for the entire set of the ozone isotopologues. This corresponds to about 97% of the dissociation threshold $D_0(^{18}O_3)$ estimated at 8620 cm^{-1}. For the main isotopologue $^{16}O_3$ such vibrational state was not yet experimentally measured. It was predicted at 8422 cm^{-1}, that is by 450 cm^{-1} higher in energy than for $^{18}O_3$, whereas the [26,7,20](7.0.1) $^{16}O_3$ level would fall in the continuum above the first dissociation threshold [82]. This means that spectra of heavy isotopic species bring new information of the molecular properties near D_0, which is not directly accessible by the bound state transitions of the main isotopologue. This experimental information could be important for the study of the deviations from the Born-Oppenheimer approximation [83-85]. Let us remind that the highest rotationally resolved absorption band of $^{16}O_3$ observed in the previous work [38] extended up upper state $(E^{obs})_{max}$ = 8277.3 cm^{-1} for the level $[J,K_a,K_c](v_1.v_2.v_3)$= [25,3,22](6.1.1).

On the theoretical side, the analyses at this energy range is not a trivial task: note that even for stable molecules with fewer number of electrons, like water isotopologue HDO, an assignment of all observed vibrational states near D_0 is not yet fully achieved [86].

It is remarkable that predictions near D_0 from *ab initio* PES [19] remain valid for the heavy ozone isotopologue with the uncertainty about one wavenumber as shown in Table II.

Rotational v-dependent constants are also in a good agreement. The (7.0.1) upper state accessible by the transitions observed in the present work corresponds to the dominant bound symmetric stretch vibration. Contrary to the case of the (1.6.3) state representing a combination of the bending angular motion and asymmetric stretch, which was discussed for $^{16}O_3$ in the previous work [38], it does not point towards another potential well and is not expected to be sensitive to the three-well interactions [42].

Another conclusion of our experiments is that the ro-vibrational transition within the ground electronic states are superposed with strong diffuse absorption features corresponding to hot vibronic bands towards triplet electronic state $^3A_2$. Consequently, in this high-energy range the vibration-rotation lines are not fully blended only in relatively restricted windows. Future work will be necessary to extend to $^{18}O_3$ the theoretical calculations [68] and experimental analyses [87] for the vibronic hot Wulf band system, which has been recently reported in the range for $^{16}O_3$.

Acknowledgements

The supports from the Russian Science Foundation (project RNF-19-12-00171) and CNRS (France) in the frame of the International Research Project SAMIA with IAO-Tomsk and from are acknowledged. We are grateful to S. Tashkun (IAO Tomsk, Russia) for collaboration in software development.

References

=== isotopic anomalies ==

[1] Krankowsky D, Mauersberger K. Heavy ozone –a difficult puzzle to solve. Science 1996;274:1324.

[2] Thiemens MH. The mass-independent ozone isotope effect. Science 2001;293(5528):226.

[3] Gao YQ, Marcus RA. Strange and unconventional isotope effects in ozone formation. Science 2001;293:259−63.
[4] Janssen C, Guenther J, Krankowsky D, Mauersberger K. Temperature dependence of ozone rate coefficients and isotope fractionation in $^{16}O-^{18}O$ oxygen mixtures. Chem Phys Lett 2003;367:34−8.
[5] Mauersberger K, Krankowsky D, Janssen C, Schinke R. Assessment of the ozone isotopic effect. Advances in atomic, molecular, and optical physics. V. 50, 54 pages (2005).
[6] Thiemens MH. History and applications of the mass-independent isotope effects. Ann Rev Earth Planet Sci 2006;34:217.
[7] Janssen C, Marcus R. Does symmetry drive isotopic anomalies in ozone isotopomer formation? Science 2001;294:951.
[8] Haverd V, Toon GC, and Griffith DWT. Evidence for altitude-dependent photolysis-induced ^{18}O isotopic fractionation in stratospheric ozone. Geophys Res Lett 2005;32:L22808.
[9] Schinke R, Grebenshchikov SY, Ivanov M, Fleurat-Lessard P. Dynamical studies of the ozone isotope effect: A status report. Annu Rev Phys Chem 2006;57:625−61.
[10] Marcus RA. Theory of mass-independent fractionation of isotopes, phase space accessibility, and a role of isotopic symmetry. PNAS 2013;110(44):11703−07.

=== isotopic exchange ===

[11] Anderson SM, Klein FS, Kaufman K. Kinetics of the isotope exchange reaction of ^{18}O with NO and O_2 at 298 K. J Chem Phys 1985;83:1648−56.
[12] Fleurat-Lessard P, Grebenshchikov SY, Schinke R, Janssen C, Krankowsky D. Isotope dependance of the $O+O_2$ exchange reaction: experiment and theory. J Chem Phys 2003;119:4700.
[13] Van Wyngarden AL, Mar KA, Boering KA, Lin JJ, Lee YT, Lin S-Y, Guo H, Lendvay G. Nonstatistical behavior of reactive scattering in the $^{18}O + {}^{32}O_2$ isotope exchange reaction. J Am Chem Soc 2007;129:2866−70.
[14] Sun Z, Yu D, Xie W, Hou J, Dawes R, Guo H. Kinetic isotope effect of the $^{16}O+{}^{36}O_2$ and $^{18}O+{}^{32}O_2$ isotope exchange reactions: Dominant role of reactive resonances revealed by an accurate time-dependent quantum wavepacket study. J Chem Phys 2015;142:174312.
[15] Guillon G, Honvault P, Kochanov R, Tyuterev Vl. First-principles computed rate constant for the $O+O_2$ isotopic exchange reaction now matches experiment. J Phys Chem Lett 2018;9:1931−6.
[16] Honvault P, Guillon G, Kochanov R, Tyuterev V. Quantum mechanical study of the $^{16}O+{}^{18}O{}^{18}O \Rightarrow {}^{16}O{}^{18}O+{}^{18}O$ exchange reaction: Integral cross sections and rate constants. J Chem Phys 2018;149(21):214304.
[17] Yuen CH, Lapierre D, Gatti F, Kokoouline V, Tyuterev VlG. The role of ozone vibrational resonances in the isotope exchange reaction $^{16}O{}^{16}O+{}^{18}O \rightarrow {}^{18}O{}^{16}O+{}^{16}O$: The time-dependent picture. J Phys Chem A, 2019;123(36):7733–43.

== ab initio ==

[18] Siebert R, Fleurat-Lessard P, Schinke R, Bittererova M, Farantos S. The vibrational energies of ozone up to the dissociation threshold: Dynamics calculations on an accurate potential energy surface. J Chem Phys 2002;116:9749–67.
[19] Tyuterev VlG, Kochanov RV, Tashkun SA, Holka F, Szalay P. New analytical model for the ozone electronic ground state potential surface and accurate ab initio vibrational predictions at high energy range. J Chem Phys 2013;139:134307.

[20] Dawes R, Lolur P, Li A, Jiang B, Guo H. Communication: An accurate global potential energy surface for the ground electronic state of ozone. J Chem Phys 2013;139:201103.
[21] Tyuterev Vl, Kochanov R, Tashkun S. Accurate *ab initio* dipole moment surface of ozone: First-principle intensity predictions for rotationally resolved spectra in a large range of overtone and combination bands. J Chem Phys 2017;146(6):064304.
[22] Tyuterev Vl, Barbe A, Mikhailenko S, Starikova E, Babikov Y. Towards the intensity consistency of the ozone bands in the infrared range: *ab initio* corrections to the S&MPO database. J Quant Spectrosc Radiat Transfer 2021;272:107801. https://doi.org/10.1016/j.jqsrt.2021.107801

=== TF 666 ==========

[23] Birk M, Wagner G, Gordon IE, Drouin BJ. Ozone intensities in the rotational bands. J Quant Spectrosc Radiat Transfer 2019:226:60. DOI: 10.1016/j.jqsrt.2019.01.004
[24] Tyuterev VlG, Barbe A, Jacquemart D, Janssen C, Mikhailenko S, Starikova E. Ab initio predictions and laboratory validation for consistent ozone intensities in the MW, 10 and 5 micron range. J Chem Phys 2019;150:184303.
[25] Mikhailenko S, Barbe A. High resolution infrared spectrum of $^{16}O_3$: The 3600-4300 cm^{-1} range reinvestigated. J Quant Spectrosc Radiat Transfer 2020;244:106823. DOI : 10.1016/j.jqsrt.2019.106823
[26] Janssen C, Boursier C, Elandaloussi H, Jeseck P, Koshelev D, Marie-Jeanne P, Rouillé C, Jacquemart D, Thibout F, Vaudescal-Escudier M, Te Y. Multi-spectral investigation of ozone: Part I. Setup & uncertainty budget. J Quant Spectrosc Radiat Transfer, HITRAN special issue, 2021.
[27] Birk M, Wagner G, Barbe A, De Backer M-R, Rotger M, Flaud J-M. ESA SEOM-IAS – Measurement and line parameter database O_3 MIR region. Zenodo 2021. DOI: 10.5281/zenodo.4428825
[28] Barbe A, Mikhailenko S, Starikova E, Tyuterev V. Infrared spectra of $^{16}O_3$ in the 900 - 5600 cm^{-1} range revisited: empirical corrections to the S&MPO and HITRAN2020 line lists. J Quant Spectrosc Radiat Transfer 2021, in press (https://doi.org/10.1016/j.jqsrt.2021.107936)

== databases

[29] Gordon IE, Rothman LS, Hargreaves RJ, et al, The HITRAN2020 molecular spectroscopic database, J Quant Spectrosc Radiat Transfer 2021, in press (https://doi.org/10.1016/j.jqsrt.2021.107949)
[30] Delahaye T, Armante R, Scott NA, Jacquinet-Husson N, Chédin A, Doue V, et al. The 2020 edition of the GEISA spectroscopic database. J Mol Spectrosc 2021, 380 (2021) 111510. Doi : 10.1016/j.jms.2021.111510
[31] Babikov Y, Mikhailenko S, Barbe A, Tyuterev VlG. S&MPO – An information system for ozone spectroscopy on the WEB. J Quant Spectrosc Radiat Transfer 2014;145:169–96. (http://www.ozone.univ-reims.fr and http://ozone.iao.ru)
[32] Albert D, Antony BK, Ba YA, Babikov YL, et al. A decade with VAMDC: Results and ambitions. Atoms 2020;8(4):76. DOI: 10.3390/atoms8040076

== Laser + CRDS==666

[33] Wenz H, Demtröder W, Flaud JM, Highly sensitive absorption spectroscopy of the ozone molecule around 1.5 μm. J Mol Spectrosc 2001;209:267–77.

[34] Campargue A, Kassi S, Romanini D, Barbe A, De Backer-Barilly MR, Tyuterev VlG. CW-cavity ring down spectroscopy of the ozone molecule in the 6625-6830 cm^{-1} region. J Mol Spectrosc 2006;240(1):1−13. https://doi.org/10.1016/j.jms.2006.07.010
[35] Campargue A, Barbe A, De Backer-Barilly M-R, TyuterevVl G and Kassi S. The near infrared spectrum of ozone by CW-cavity ring down spectroscopy between 5850 and 7000 cm^{-1}: new observations and exhaustive review. Phys Chem Chem Phys 2008;10:2925–46.
[36] Barbe A, Mikhailenko S, Starikova E, De Backer-Barilly M-R, Tyuterev VlG, Mondelain D, Kassi S, Campargue A, Janssen C, Tashkun S, Kochanov R, Gamache R, Orphal J. Ozone spectroscopy in the electronic ground state: High resolution spectra analyses and update of line parameters since 2003. J Quant Spectrosc Radiat Transfer 2013;130:172–90.
[37] Campargue A, Kassi S, Mondelain D, Barbe A, Starikova E, De Backer MR, Tyuterev VlG. Detection and analysis of three highly excited vibrational bands of $^{16}O_3$ by CW-CRDS near the dissociation threshold. J Quant Spectrosc Radiat Transfer 2015;152:84–93. https://doi.org/10.1016/j.jqsrt.2014.10.019
[38] Vasilchenko S, Barbe A, Starikova E, Kassi S, Mondelain D, Campargue A, Tyuterev V. Detection and assignment of ozone bands near 95% of the dissociation threshold: ultra-sensitive experiments for probing potential energy function and vibrational dynamics. Phys Rev A, 2020;102(5):052804. DOI: 10.1103/PhysRevA.102.052804

= Do + reef ===

[39] B Ruscic, Unpublished results obtained from active thermochemical tables (ATcT) based on the Core (Argonne), Thermochemical Network version 1.110, 2010. available at atct.anl.gov.
[40] Holka, F.; Szalay, P. G.; Muller, T.; Tyuterev, V. G. Toward an improved ground state potential energy surface of ozone. J. Phys.Chem. A 2010, 114, 9927−9935.
[41] Tyuterev VlG, Kochanov R, Campargue A, Kassi S, Mondelain D, Barbe A, et al. Does the “Reef Structure” at the Ozone Transition State towards the Dissociation Exist? New Insight from Calculations and Ultrasensitive Spectroscopy Experiments. Phys Rev Lett 2014;113:143002. https://doi.org/10.1103/PhysRevLett.113.143002
[42] Kokoouline V, Lapierre D, Alijah A, Tyuterev V. Localized and delocalized bound states of the main isotopologue $^{48}O_3$ and of ^{18}O-enriched $^{50}O_3$ isotopomers of the ozone molecule near the dissociation threshold. Phys Chem Chem Phys 2020;**22**:15885–99.
[43] Dawes, R.; Lolur, P.; Ma, J.; Guo, H. Communication: Highly accurate ozone formation potential and implications for kinetics. J.Chem. Phys. 2011, 135, 081102.

== 668/688/ ===
[44] Mondelain D, Campargue A, Kassi S, Barbe A, Starikova E, De Backer MR, Tyuterev VlG. The CW-CRDS spectra of the $^{16}O/^{18}O$ isotopologues of ozone between 5930 and 6340 cm^{-1}. Part 1: $^{16}O^{16}O^{18}O$. J Quant Spectrosc Radiat Transfer 2013;116:49–66.
[45] Starikova E, Barbe A, De Backer MR, Tyuterev VlG, Mondelain D, Kassi S, Campargue A. Three new bands of $^{18}O^{16}O^{18}O$ by CW-CRDS between 6340 and 6800 cm^{-1}. J Quant Spectrosc Radiat Transfer 2014;149:211–18.
[46] De Backer MR, Barbe A, Starikova E, Tyuterev VlG, Mondelain D, Kassi S, Campargue A. The CW-CRDS spectra of the $^{16}O/^{18}O$ isopotologues of ozone between 5930 and 6340 cm^{-1}. Part 3: $^{16}O^{18}O^{18}O$ and $^{18}O^{16}O^{18}O$. J Quant Spectrosc Radiat Transfer 2013;127:24–36.

[47] Barbe A, Starikova E, De Backer MR, Tyuterev VlG. Analyses of infrared spectra of asymmetric ozone isopotologue $^{16}O^{16}O^{18}O$ in the range 950-3850 cm^{-1}. J Quant Spectrosc Radiat Transfer 2018;218:231–47.
[48] Starikova E, Barbe A, De Backer MR, Tyuterev V. Analysis of thirteen absorption bands of $^{16}O^{18}O^{18}O$ ozone isotopomer in the 950–3500 cm^{-1} infrared spectral range. J Quant Spectrosc Radiat Transfer 2020;257:107364. DOI: 10.1016/j.jqsrt.2020.107364

====888 TF======

[49] Perrin A, Vasserot AM, Flaud JM, Camy-Peyret C, Rinsland CP, Smith MAH, Malathy Devi V. The v_2 bands of $^{18}O_3$, $^{18}O^{16}O^{18}O$, and $^{16}O^{18}O^{18}O$: Line positions and intensities. J Mol Spectrosc 1990;143:311–17. (doi:10.1016/0022-2852(91)90095-R)
[50] Flaud JM, Camy-Peyret C, Malathy Devi V, Rinsland CP, Smith MAH. The v1 and v3 bands of $^{18}O_3$ and $^{18}O^{16}O^{18}O$: Line positions and intensities. J Mol Spectrosc 1987;122:221–228. (doi:10.1016/0022-2852(87)90231-1)
[51] Chichery A, Barbe A, Tyuterev VlG, Bourgeois MT, Analysis of High-Resolution Spectra of $^{18}O_3$. 1. Spectral Range 1300-3100 cm^{-1}. J Mol Spectrosc 2001;206:1–13. (doi:10.1006/jmsp.2000.8283)
[52] Chichery A, Barbe A, Tyuterev VlG, Analysis of high-resolution spectra of $^{18}O_3$. 2. Spectral range 3100-4900 cm^{-1}. J Mol Spectrosc 2001;206:14–26. (doi:10.1006/jmsp.2000.8284)

====888crds======

[53] Campargue A, Liu AW, Kassi S, De Backer-Barilly M-R, Barbe A, Starikova E et al. CW-Cavity Ring Down spectroscopy of $^{18}O_3$. Part 1: Experiment and analysis of the 6200-6400 cm^{-1} spectral region. J Mol Spectrosc 2009;255:75–87.
[54] Starikova E, De Backer-Barilly M-R, Barbe A, Tyuterev VlG, Campargue A, Liu AW, et al. CRDS spectroscopy of $^{18}O_3$. Part 2: Analysis of six interacting bands between 5930 and 6080 cm^{-1}. J Mol Spectrosc 2009;255:144–56.
[55] Starikova E, Barbe A, Tyuterev VlG, De Backer-Barilly MR, Kassi S, Campargue A. CW-Cavity Ring Down Spectroscopy of $^{18}O_3$. Part 3: Analysis of the 6490–6900 cm^{-1} region and overview comparison with the $^{16}O_3$ main isotopologue. J Mol Spectrosc 2009;257:40–56.
[56] Starikova E, Barbe A, De Backer-Barilly MR, Tyuterev VlG, Mondelain D, Kassi S, Campargue A. Analysis of the CRDS spectrum of $^{18}O_3$ between 6950 and 7125 cm^{-1}. J Quant Spectrosc Radiat Transfer 2012;113:1741–52.
[57] Starikova EN, Barbe A, De Backer-Barilly MR, Tyuterev VlG, Tashkun SA, Kassi S, et al. Isotopic shifts in vibration levels of ozone due to homogeneous substitution: Band centres of $^{18}O_3$ derived from analysis of CW-CRDS spectra in the 5900-7000 cm^{-1} range. Chem Phys Lett 2009;470:28–34
[58] Starikova E, Mondelain D, Barbe A, Tyuterev VlG, Kassi S, Campargue A, CRDS detection and modelling of vibrational bands of $^{18}O_3$ approaching the dissociation threshold (7400–7920 cm^{-1}). J Quant Spectrosc Radiat Transfer 2015;161:203–14.
[59] Vasilchenko S, Kassi S, Mondelain D, Campargue A. High-Resolution Laser Spectroscopy of the Ozone Molecule at the Dissociation Threshold, Amospheric and Oceanic Optics, 2021, *to be published*

=== electronic===

[60] Mondelain D, Kassi S, Jost R, Campargue A. The high sensitivity absorption spectrum of ozone ($^{18}O_3$ and $^{16}O_3$) near 7800 cm^{-1}: identification of the $^3A_2(000)$-X(110) hot band superimposed to very weak vibrational bands. Chem Phys Letters 2011;510:191–6.
[61] Mondelain D, Jost R, Kassi S, Judge RH, Tyuterev VlG, and Campargue A. Predissociaton and spectroscopy of the $^3A_2(000)$ state of $^{18}O_3$ from CRDS spectra of the $^3A_2(000)$ ← $X^1A_1(110)$ hot band near 7900 cm^{-1}. J Quant Spectrosc Radiat Transfer 2012;113:840–49.

=== experimental ==

[62] Konefał M, Kassi S, Mondelain D, Campargue A. High sensitivity spectroscopy of the O_2 band at 1.27 μm: (I) pure O_2 line parameters above 7920 cm^{-1}. J Quant Spectrosc Radiat Transf 2020;241:106653. https://doi.org/10.1016/j.jqsrt.2019.106653.
[63] Griggs M. Absorption coefficients of ozone in the ultraviolet and visible regions. J Chem Phys 1968;49(2):857–59. https://doi.org/10.1063/1.1670152.

=== *wulf* ==========
[64] Grebenshchikov SYu, Qu Z-W, Zhuz H, Schinke R. New theoretical investigations of the photodissociation of ozone in the Hartley, Huggins, Chappuis, and Wulf bands. Phys Chem Chem Phys 2007;9:2044–64. https://doi.org/10.1039/B701020F
[65] Günther J, Anderson SM, Hilpert G, Mauersberger K. Rotational structure in the absorption spectra of $^{18}O_3$ and $^{16}O_3$ near 1 μm: A comparative study of the $^3A_2$ and $^3B_2$ states. J Chem Phys 1998;108:5449. https://doi.org/10.1063/1.475933
[66] Bacis R, Bouvier AJ, Flaud JM. The ozone molecule: electronic spectroscopy. Spectrochim Acta Part A 1998;54:17–34. https://doi.org/10.1016/S1386-1425(97)00259-X
[67] Wannous G, Bouvier AJ, Helou ZEl, Chillier X, Churassy S, Bacis R, Campargue A, Weirauch G, Judge RH. Contribution to the analysis of the predissociated rovibronic structure of the symmetric isotopomers $^{16}O_3$ and $^{18}O_3$ of ozone near 10,400 cm^{-1}: $^3A_2$ (3^2_0)←$X^1A_1(0^0_0)$ and $^3B_2$←X^1A_1. Spectrochim Acta Part A 2004;60:889–98. https://doi.org/10.1016/S1386-1425(03)00316-0
[68] Egorov O, Valiev RR, Kurten T, Tyuterev Vl. Franck-Condon factors and vibronic patterns of singlet-triplet transitions of $^{16}O_3$ molecule falling near the dissociation threshold and above. J Quant Spectrosc Radiat Transfer 2021;273:107834. DOI: 10.1016/j.jqsrt.2021.107834
[69] Gordon IE, Rothman LS, Hill C, Kochanov RV, et al. The HITRAN2016 molecular spectroscopic database. J Quant Spectrosc Radiat Transf 2017;203:3–69. https://doi.org/10.1016/j.jqsrt.2017.06.038.
[70] Furtenbacher T, Tóbiás R, Tennyson J, Polyansky OL, Kyuberis AA, Ovsyannikov RI, et al. The W2020 database of validated rovibrational experimental transitions and empirical energy levels of water isotopologues. II. $H_2{}^{17}O$ and $H_2{}^{18}O$ with an Update to $H_2{}^{16}O$. J Phys Chem Ref Data 2020;49:43103. https://doi.org/10.1063/5.0030680.
[71] Huang X, Schwenke DW, Freedman RS, Lee TJ. Ames-2016 line lists for 13 isotopologues of CO_2: Updates, consistency, and remaining issues. J Quant Spectrosc Radiat Transf 2017;203:224–41. https://doi.org/10.1016/J.JQSRT.2017.04.026.
[72] Tyuterev VlG, Tashkun SA, Seghir H. High-order contact transformations: General algorithm, computer implementation and triatomic tests. SPIE Proc Ser 2004;5311:164–75. https://doi.org/10.1117/12.545641
[73] Tyuterev VlG, Tashkun SA, Rey M, Kochanov RV, Nikitin AV, Delahaye T. Accurate spectroscopic models for methane polyads derived from a potential energy surface using high-order Contact Transformations. J Phys Chem A. 2013;117:13779–805.

[74] Flaud JM, Bacis R. The ozone molecule: infrared and microwave spectroscopy. Spectrochim Acta Part A 1998;54:3–16. https://doi.org/10.1016/S1386-1425(97)00214-X
[75] Tyuterev VlG, Kochanov RV, Tashkun SA. Analytical representation for the ozone electronic ground state potential function in the spectroscopically accessible range and extended vibration predictions. In: Proceedings of XVII international symposium HighRus-2012 (http://symp.iao.ru/ru/hrms/17/proceedings)
[76] Plateaux J-J, Régalia L, Boussin C, Barbe A. Multispectrum fitting technique for data recorded by Fourier transform spectrometer: application to N_2O and CH_3D. J Quant Spectrosc Radiat Transfer 2001;68:507–20.
[77] Chichery A. «*Analyse des spectres infrarouges haute résolution des formes isotopiques de l'ozone. Application aux études atmosphériques*». PhD thesis, Université de Reims, 2000.
[78] Taskhun SA, Tyuterev VlG. GIP: A program for experimental data reduction in molecular spectroscopy. SPIE Proc Ser 1994;2205:188–91. https://doi.org/10.1117/12.166203
[79] Flaud JM, Camy-Peyret C. Vibration-rotation intensities in H_2O-type molecules. Application to the $2\nu_2$, ν_1, and ν_3 bands of $H_2{}^{16}O$. J Mol Spectrosc 1975;55:278–310. https://doi.org/10.1016/0022-2852(75)90270-2
[80] Watson JKG. Determination of centrifugal distortion coefficients of asymmetric-top molecules. J Chem Phys 1967;46:4189–96.
[81] Pearson JC, Müller HSP, Pickett HM, Cohen EA, Drouin BJ. Introduction to submillimeter, millimeter and microwave spectral line catalog. J Quant Spectrosc Radiat Transfer 2010;111:1614–16. DOI: 10.1016/j.jqsrt.2010.02.002
[82] Lapierre D, Alijah A, Kochanov R, Kokoouline V, Tyuterev Vl. Lifetimes and wave functions of ozone metastable vibrational states near the dissociation limit in a full-symmetry approach. Phys Rev A 2016;94(4):042514. DOI: 10.1103/PhysRevA.94.042514
[83] Garcia-Fernandez P, Bersuker IB, Boggs JE. Lost topological (Berry) phase factor in electronic structure calculations. Example: The ozone molecule. Phys Rev Lett 2006;96:163005.
[84] Alijah A, Lapierre D, Tyuterev Vl. Non-adiabatic coupling in the ozone molecule. Mol Phys 2018;116(19-20):2660–70. DOI: 10.1080/00268976.2018.1473650
[85] Tajti A, Szalay PG, Kochanov R, Tyuterev VG. Diagonal Born-Oppenheimer corrections to the ground electronic state potential energy surfaces of ozone: Improvement of ab initio vibrational band centers for the $^{16}O_3$, $^{17}O_3$, and $^{18}O_3$ isotopologues. Phys Chem Chem Phys 2020;22(42):24257–69. DOI: 10.1039/d0cp02457k
[86] Zobov NF, Koshelev MA, Makarov DS, et al. A global line list for HDO between 0 and 35000 cm^{-1} constructed using multiphoton spectra. J Quant Spectrosc Radiat Transfer 2021;271:107694. DOI: 10.1016/j.jqsrt.2021.107694
[87] Vasilchenko S, Mondelain D, Kassi S, Campargue A. Predissociation and pressure dependence in the low frequency far wing of the Wulf absorption band of ozone near 1.2 µm, J Quant Spectrosc Radiat Transfer 2021;272:107678. DOI : 10.1016/j.jqsrt.2021.107678